DNA Unwinding

DOI: 10.1002/anie.201001332

A Graphene-Based Platform for the Assay of Duplex-DNA Unwinding by Helicase**

*Hongje Jang, Young-Kwan Kim, Hyun-Mi Kwon, Woon-Seok Yeo, Dong-Eun Kim, and Dal-Hee Min**

Helicases are an important class of enzymes that unwind double-stranded nucleic acids into single-stranded ones using energy from nucleoside triphosphate (NTP) hydrolysis.[1] They have been implicated in both virus replication and cellular processes that require single-stranded nucleic acids, including DNA replication, repair, and transcription.[2] Because of their critical role in viral replication and proliferation, helicases have been targeted for therapy in many viral diseases.[3] In fact, viral helicase inhibitors have been shown to be successful drug candidates in the treatment of hepatitis C and herpes simplex virus infection.[4] Therefore, the development of a simple, fast, and cost-effective platform is important for the assay of the nucleic acid unwinding activity of helicases.

A conventional method for assessing the DNA or RNA unwinding activity of helicase involves substrates that are double-stranded nucleic acids, one of which is radiolabeled with ^{32}P. The degree of substrate unwinding by helicase can be estimated by using polyacrylamide gel electrophoresis (PAGE) and subsequent visualization of the radioisotope.[5] However, the conventional assay is time-consuming and inefficient because of the lengthy preparation time for radiolabeled substrates, which have limited shelf life, and for running PAGE. In addition, the assay method assumes that unwound single-stranded DNA (ssDNA) will not undergo reannealing to the complementary strand and that any reannealed double-stranded DNA (dsDNA), which consists of trap DNA and previously unwound complementary DNA, will not participate in the helicase reaction as substrate.[6]

Overall, the conventional assay method is not adequate for multiple-turnover helicase reactions or parallel activity screenings. To date, several other strategies for the assay of helicase activity have been developed, based on enzyme-linked immunosorbent assay (ELISA),[7] fluorescence resonance energy transfer (FRET),[8] or chemiluminescence.[9] These newer approaches partly overcome the limitations of the conventional assay but still possess undesirable features, such as high cost and laborious procedure, which prohibit their routine implementation.

Herein, we report a platform for the assay of helicase unwinding activity that relies on the preferential binding of graphene oxide (GO) to ssDNA over dsDNA, thereby quenching the fluorescence of dyes that are conjugated to ssDNA. Previously, GO was reported to interact strongly with nucleotides through π-stacking interaction between the ring structures in the nucleobases and the hexagonal cells of GO, whereas dsDNA cannot be stably adsorbed onto the GO surface because of efficient shielding of nucleobases within the negatively charged phosphate backbone of dsDNA.[10] In addition, GO is known to efficiently quench the fluorescence of nearby organic dyes.[11] The helicase assay based on GO starts with the preparation of a dsDNA substrate containing a fluorescent dye at the end of one strand. To initiate the helicase reaction, helicase is added to a mixture of dsDNA and GO in which the dsDNA exhibits intense fluorescence. As the helicase-induced unwinding of dsDNA proceeds, the fluorescence decreases because of strong interaction of GO with unwound ssDNA, which results in fluorescence quenching by GO (Figure 1).

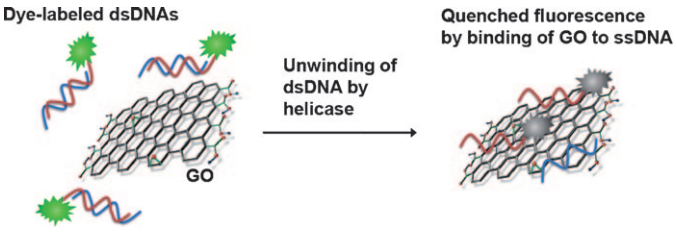

Figure 1. GO-based system for the assay of helicase unwinding activity.

To demonstrate our strategy, we used severe acute respiratory syndrome coronavirus (SARS-CoV, SCV) helicase nsP13.[12] SARS is a fatal infectious disease that develops flulike symptoms and has a high mortality rate. SCV helicase has been recognized as a potential target for the development of antiviral drugs against SARS.[13] A dsDNA substrate of SCV helicase was designed based on a previous report.[14]

[*] H. Jang, Y.-K. Kim, Prof. Dr. D.-H. Min
Department of Chemistry, Institute for the BioCentury
Korea Advanced Institute of Science and Technology (KAIST)
373-1 Guseong-dong, Yuseong-gu, Daejeon 305-701 (Korea)
Fax: (+82)-42-350-2810
E-mail: dalheemin@kaist.ac.kr
H.-M. Kwon, Prof. Dr. W.-S. Yeo, Prof. Dr. D.-E. Kim
Department of Bioscience and Biotechnology
Konkuk University
Seoul 143-701 (Korea)

[**] This work was supported by the Basic Science Research Program and Mid-career Researcher Program through the National Research Foundation of Korea (NRF) funded by the Korean government (the Ministry of Education, Science, and Technology, MEST; grant nos. 313-2008-2-C00538, 2008-0062074, and 2009-0071058), by the Nano R&D program (2008-2004457) and WCU Project (R33-10128), and by the National Honor Scientist Program.

Supporting information for this article is available on the WWW under http://dx.doi.org/10.1002/anie.201001332.

We first prepared GO according to a modified Hummer's method.[15] To confirm the successful formation of a single-layered GO sheet, the prepared GO was analyzed by atomic force microscopy (AFM). The sheet width and thickness (height) of GO were approximately 0.1–3 μm (with a few sheets larger than 4 μm) and 1.4 nm, respectively (Figure 2a,b).[16] The chemical structure of GO was characterized

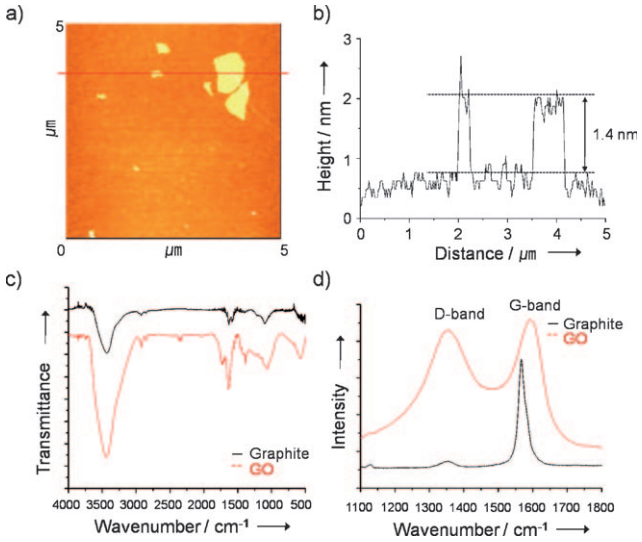

Figure 2. Characterization of GO. a) AFM image and b) height profile of GO showing the dimensions of prepared GO as 0.1–3 μm in width and ca. 1.4 nm in height. c) IR and d) Raman spectra of GO, which present characteristic peaks corresponding to oxygen-containing functional groups and disordered sp^2 structures in GO, respectively.

by both IR and Raman spectroscopy. Several characteristic peaks of functional groups containing oxygen were observed in the IR spectrum of GO, including peaks at 1716 and 1079 cm^{-1} that resulted from C=O and C–O stretching, respectively (Figure 2c). Strong D-band absorption at 1350 cm^{-1} appeared in the Raman spectrum of GO (Figure 2d). Taken together, these data support the premise that single-layered GO sheets were successfully prepared.

We next used the dye fluorescein amidite (FAM) attached to ssDNA (F-ssDNA) and demonstrated that fluorescence quenching occurs upon binding of F-ssDNA to the GO surface. Separate mixtures containing GO (0.5 μg mL^{-1}) and either annealed F-dsDNA or F-ssDNA were prepared in helicase reaction buffer (pH 8.0 buffer containing 50 mM Tris–HCl, 50 mM NaCl, 0.25 mM ethylenediaminetetraacetic acid (EDTA), 0.65 mM $MgCl_2$, and 10% glycerol), and the fluorescence emission spectra of the mixtures were then measured over time. The F-dsDNA showed strong fluorescence around 520 nm, regardless of the presence of GO. However, a mixture of F-ssDNA and GO showed up to ≈92% quenching of fluorescence after 10 minutes at room temperature, as a result of the interaction of GO with ssDNA (Figure 3a). The dsDNA is expected to have repulsive interaction with GO because of the negative charges on GO (zeta potential of GO: −24.89 mV) and the negatively charged phosphate backbone of DNA. Quenching of fluorescence did take place over time in the F-dsDNA mixture, but the fluorescence reached a plateau at a relatively high level after 10 minutes (Figure 3b). In contrast, GO quenched nearly all of the fluorescence of F-ssDNA because of its selective interaction with ssDNA as compared to dsDNA under the experimental conditions employed.

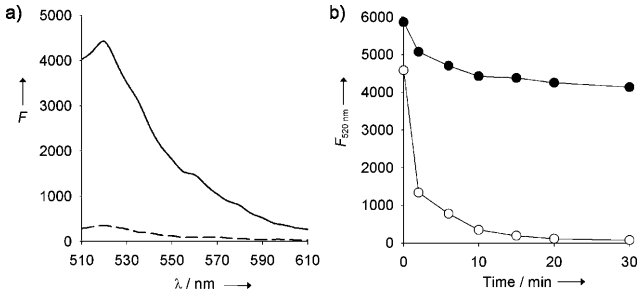

Figure 3. FAM fluorescence quenching by GO. a) Fluorescence spectra of F-dsDNA (——) and F-ssDNA (– – –) after incubation with GO for 10 min. A high degree of fluorescence quenching was observed in F-ssDNA, compared to F-dsDNA, in the presence of GO. b) Fluorescence intensities of F-ssDNA (○) and F-dsDNA (●) in the presence of GO measured at 520 nm at various time intervals. Quenching of fluorescence occurred over time and ca. 92% of the quenching was achieved within the first 10 min. Figures S1 and S2 in the Supporting Information show the results of experiments that were performed to find the optimum concentrations of GO and F-dsDNA.

We then measured SCV helicase activity using F-dsDNA as a substrate in the presence of GO, with various concentrations of the helicase. Mixtures of F-dsDNA, GO, and SCV helicase in reaction buffer containing adenosine 5′-triphosphate (ATP, 10 mM) were prepared and incubated at 37 °C. The fluorescence emission at 520 nm was measured at various time intervals. As expected, the degree of F-dsDNA unwinding by helicase depended on the helicase concentration (Figure 4a). To confirm that the fluorescence quenching resulted from F-dsDNA unwinding by helicase, the concentration of ATP—an energy source for helicase activity—was varied, while the concentration of helicase was kept constant

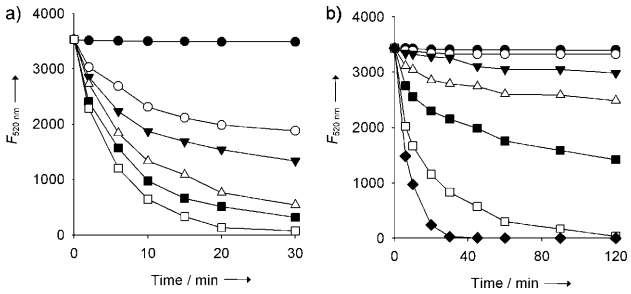

Figure 4. F-dsDNA unwinding activity assays were performed with various concentrations of a) SCV helicase and b) ATP. a) [Helicase] (in nM): ● 0; ○ 0.625; ▼ 1.25; △ 2.5; ■ 5; □ 10. b) [ATP] (in mM): ● 0; ○ 0.1; ▼ 0.5; △ 1; ■ 2; □ 5; ◆ 10. Unwinding activity was dependent on the concentrations of helicase and ATP, as expected. The GO-based platform made feasible quantitative measurements of helicase reactions with excess amounts of substrate (100 nM). Fluorescence spectra corresponding to all the data points are shown in Figures S3 and S4 in the Supporting Information.

at 10 nM. Helicase activity did indeed increase as the ATP concentration was raised (Figure 4b).

Next, we performed assays of helicase inhibition to demonstrate that the present method is quantitative and robust enough for general applications, including inhibitor assays. Two compounds, 5′-adenylimidodiphosphate (AMP-PNP) and doxorubicin (also known as hydroxydaunorubicin), were chosen as model inhibitors of helicase. AMP-PNP, a nonhydrolyzable ATP analogue, was previously reported to inhibit helicase activity by competing for the ATP binding site.[17] Doxorubicin, an anticancer agent, intercalates with duplex DNA, thereby slowing down the unwinding of dsDNA.[18] We began with reaction mixtures containing helicase (10 nM), F-dsDNA (100 nM), GO (1 $\mu g\,mL^{-1}$), ATP (10 mM), and various concentrations of the inhibitors in helicase reaction buffer. In the case of doxorubicin, mixtures of F-dsDNA and doxorubicin were prepared and incubated for 20 minutes at room temperature, prior to mixing with the other reagents, to ensure the intercalation of doxorubicin with F-dsDNA without interference from the other components. The change in fluorescence intensity at 520 nm was then measured for 30 minutes at 37 °C for each of the reaction mixtures.

The half maximal inhibitory concentration (IC_{50}) values of AMP-PNP and doxorubicin were found to be 480.9 and 31.3 mM, respectively (Figure 5a,b). To perform high-throughput screening of inhibitors, it would be efficient to be able to measure helicase activities from fluorescence images of multiwell plates containing multiple reaction mixtures. To demonstrate the feasibility of parallel assays, the inhibition assays were carried out in a 96-well plate for 30 minutes at 37 °C, and fluorescence images were obtained from the reaction mixtures in the plate using an IVIS imaging system (Xenogen, Alameda, CA, USA). The inhibition of helicase activity by AMP-PNP and doxorubicin was clearly visualized, and dose dependency was distinctly observable in the fluorescence images (Figure 5c).

Finally, we performed a conventional helicase assay using ^{32}P-labeled dsDNA for direct comparison with the present assay. The ^{32}P-labeled dsDNA substrate was first prepared using [γ-^{32}P]ATP and T4 polynucleotide kinase, followed by annealing, according to established procedure. The reaction mixture containing ^{32}P-labeled dsDNA (10 nM), helicase (100 nM), and trap DNA (10 μM) was prepared in a reaction buffer. Trap DNA (unlabeled bottom-strand DNA) was required in excess to prevent the reannealing of the unwound, labeled DNA products. Aliquots were taken after 10 and 30 minutes, quenched by adding the quench buffer (100 mM EDTA at pH 8.0, 0.4% sodium dodecyl sulfate, 20% (v/v) glycerol, and 1% bromophenol blue) and analyzed immediately by electrophoresis in nondenaturing 10% polyacrylamide gel (Figure 6a, top). As a control, heat-denatured DNA was prepared in the presence of trap DNA and included in the gel. The gel image obtained by a phosphorimager gives the relative amounts of dsDNA and ssDNA in each sample.

Basically, the gel-based assay is an endpoint assay that can be analyzed only after the reaction is terminated. This feature makes the gel-based assay inappropriate for real-time kinetics studies. The data also illustrate the requirement for trap DNA

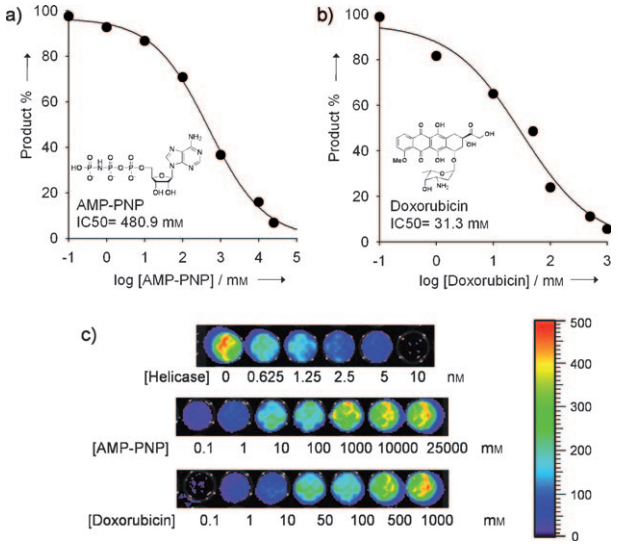

Figure 5. Dose-dependent inhibition of helicase reactions was carried out using the GO-based method. a,b) Inhibition of helicase by a) AMP-PNP (nonhydrolyzable ATP derivative) and b) doxorubicin (anthracycline anticancer agent) was observed and IC_{50} values were obtained. c) Fluorescence images of the reaction mixtures of helicase, F-dsDNA, and GO were obtained in the absence and presence of the inhibitors. The image in the first row shows that duplex-DNA unwinding is dependent on the helicase concentration. Quantitative inhibition assays were also performed with AMP-PNP and doxorubicin using a fluorescence imager, and demonstrated that a high-throughput assay is readily feasible (second and third rows).

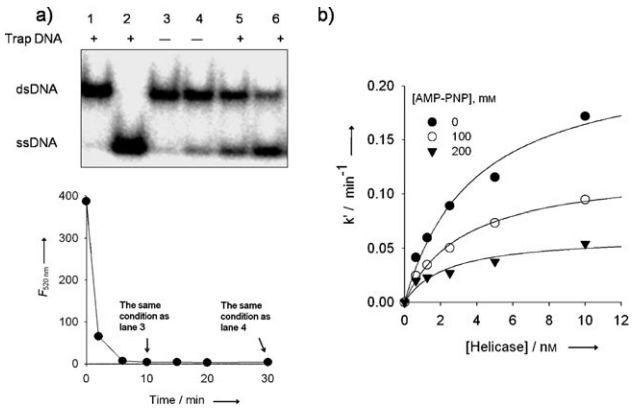

Figure 6. Comparison of a conventional ^{32}P-based helicase assay and the GO-based assay. a) Native-gel shift assay of helicase unwinding of dsDNA substrate was performed by resolving unwound DNA on a native PAGE and visualizing with a phosphorimager. Lane 1: substrate dsDNA; lane 2: heat-denatured control; lanes 3 and 5: unwinding reaction for 10 min; lanes 4 and 6: unwinding reaction for 30 min. The data illustrate the requirement for trap DNA in the conventional assay. The PAGE-based assay is a kind of endpoint assay, whereas the GO-based assay is performed in real time. Top: GO-based assay of helicase unwinding of dsDNA substrate was performed for comparison with conventional assay. Bottom: Fluorescence was completely quenched within 10 min. b) Inhibition of helicase by AMP-PNP was quantitatively measured as the helicase concentration changed. The GO-based assay made helicase inhibition kinetics straightforward, since this assay is based on quantitative and real-time measurements.

because equal time periods of unwinding did not exhibit the same amount of unwound product (ssDNA) in the presence, versus the absence, of trap DNA. In contrast, the present GO-based method (Figure 6a, bottom) shows that unwinding of dsDNA was completed within 10 minutes under similar conditions even in the absence of trap DNA. This result indicates that the GO-based method substantiates a condition for preventing reannealing of the unwound ssDNA by capturing the displaced ssDNA efficiently. Reannealing of the unwound ssDNA causes less accumulation of ssDNA products at a given time than that performed in the presence of an appropriate trap molecule. Thus, the absence of trap DNA is not adequate to reflect accumulation of ssDNA products. More importantly, the conventional gel-based DNA unwinding assay is simply an all-or-none method that reports only the completely unwound ssDNA product, whereas the GO method can report progress of dsDNA unwinding in real time. Because an excess of trap DNA is needed for precise measurement in the conventional assay method, the cost of the assay is increased substantially, thus hampering the use of parallel assays and multiple samples. In contrast, the present method is a fluorescence-based assay, which can be monitored in real time under various reaction conditions.

To illustrate the power of this method, the kinetics of helicase inhibition, with AMP-PNP as inhibitor, was measured by following the fluorescence intensity, as a function of time, of reaction mixtures containing various concentrations of helicase and AMP-PNP. Based on our assay method, the relative rates of unwinding of dsDNA by helicase could be calculated (Figure 6b). The GO-based assay platform allows quantitative measurement of helicase activity in real time, thus making it more applicable to studies of helicase inhibition kinetics than the conventional gel-based assay.

In conclusion, we have developed a new GO-based platform for the assay of duplex-DNA unwinding activity. To the best of our knowledge, this work is the first to utilize GO for an enzyme activity assay. The GO-based platform has several advantages over the conventional method. First, the helicase activity can be monitored in real time by following the change in fluorescence, without requiring any additional steps or reagents. Second, the GO-based assay is cost-effective compared to the conventional assay, which demands expensive isotope labeling and trap DNA. The GO, a critical component in the present method, can be prepared in large quantities from graphite available at very low cost. Third, the prepared GO has a much longer shelf life than ^{32}P, which has a half-life of only 14 days. Under ambient conditions, GO can be stored for months in the form of a suspended aqueous solution, or considerably longer in powder form. Fourth, the present method makes high-throughput screening feasible. As shown in Figure 5, fluorescence imaging of multiple samples makes possible parallel assays, without the need for any further purification or resolving steps. Therefore, this platform can be easily applied to any high-throughput analysis system. We expect that this method will be readily applicable to any research involving duplex-DNA unwinding, and to the screening of helicase inhibitors as drug candidates in antivirus therapy. Such studies will benefit from the method's quantitativeness, cost-effectiveness, and technical simplicity.

Experimental Section

The GO sheets were prepared according to previously reported methods.[15] SARS-CoV helicase was overexpressed in *Escherichia coli* and purified as described previously.[19] Then upper-strand DNA (12 μL, 10 μM; 5′-TTT TTT TTT TTT TTT GAG CGG ATT ACT ATA CTA CAT TAG AAT TCC-3′, Genotech, Seoul, Korea) and fluorescent-dye-conjugated bottom-strand DNA (6 μL, 10 μM; 5′-FAM-GGA ATT CTA ATG TAG TAT AGT AAT CCG CTC-3′, Genotech) were mixed and annealed in pH 8.0 buffer containing 50 mM Tris–HCl and 50 mM NaCl (1 × buffer). Substrate solution was prepared by mixing annealed substrate (0.2 μM), EDTA (0.5 mM; Bio-Rad, Hercules, CA, USA), ATP disodium (20 mM; Sigma–Aldrich, St. Louis, MO, USA), and $MgCl_2$ (1.3 mM; Junsei, Tokyo, Japan) in 1 × buffer containing 10% glycerol solution. GO solution was prepared in 1 × buffer (1 mg mL^{-1}); the substrate solution (30 μL) and GO solution (30 μL) were mixed, and then the helicase reaction was initiated by addition of various amounts of helicase stock solution (200 nM). After the addition of helicase, the fluorescence intensity was measured by using a Synergy Mx fluorometer (BioTek, Potton, UK) at 520 nm for 30 min.

Received: March 5, 2010
Revised: April 19, 2010
Published online: July 7, 2010

Keywords: biosensors · DNA · fluorescence spectroscopy · graphene · viruses

[1] a) A. J. van Brabant, R. Stan, N. A. Ellis, *Annu. Rev. Genomics Hum. Genet.* **2000**, *1*, 409; b) S. S. Velankar, P. Soultanas, M. S. Dillingham, H. S. Subramanya, D. B. Wigley, *Cell* **1999**, *97*, 75; c) D. E. Kim, M. Narayan, S. S. Patel, *J. Mol. Biol.* **2002**, *321*, 807; d) M. R. Singleton, M. R. Sawaya, T. Ellenberger, D. B. Wigley, *Cell* **2000**, *101*, 589.

[2] a) W. L. de Laat, N. G. Jaspers, J. H. Hoeijmakers, *Genes Dev.* **1999**, *13*, 768; b) T. Lindahl, R. T. Wood, *Science* **1999**, *286*, 1897.

[3] a) A. D. Kwong, B. G. Rao, K. T. Jeang, *Nat. Rev. Drug Discovery* **2005**, *4*, 845; b) C. S. Crumpacker, P. A. Schaffer, *Nat. Med.* **2002**, *8*, 327; c) P. S. Jones, *Antiviral Chem. Chemother.* **1998**, *9*, 283; d) D. N. Frick, *Drug News Perspect.* **2003**, *16*, 355; e) X. G. Xi, *Curr. Med. Chem.* **2007**, *14*, 883.

[4] a) G. Kleymann, R. Fischer, U. A. K. Betz, M. Hendrix, W. Bender, U. Schneider, G. Handke, P. Eckenberg, G. Hewlett, V. Pevzner, J. Baumeister, O. Weber, K. Henniger, J. Keldenich, A. Jensen, J. Kolb, U. Bach, A. Popp, J. Maben, I. Frappa, D. Haebich, O. Lockhoff, H. Rubsamen-Waigmann, *Nat. Med.* **2002**, *8*, 392; b) J. J. Crute, C. A. Grygon, K. D. Hargrave, B. Simoneau, A. M. Faucher, G. Bolger, P. Kibler, M. Liuzzi, M. G. Cordingley, *Nat. Med.* **2002**, *8*, 386.

[5] P. Borowski, A. Niebuhr, O. Mueller, M. Bretner, K. Felczak, T. Kulikowski, H. Schmitz, *J. Virol.* **2001**, *75*, 3220.

[6] The trap DNA is a ssDNA lacking any fluorescent or radioisotope label, which is complementary to the displaced strand of DNA. Trap DNA is generally added in excess to the helicase reaction mixture to prevent reannealing of unwound, labeled DNA, which would result in going back to substrate dsDNA. See R. L. Eoff, K. D. Raney, *Nat. Struct. Mol. Biol.* **2006**, *13*, 242.

[7] a) C. C. Hsu, L. H. Hwang, Y. W. Huang, W. K. Chi, Y. D. Chu, D. S. Chen, *Biochem. Biophys. Res. Commun.* **1998**, *253*, 594; b) O. Artsaenko, K. Tessmann, M. Sack, D. Haussinger, T. Heintges, *J. Gen. Virol.* **2003**, *84*, 2323.

[8] I. Rasnik, S. Myong, T. Ha, *Nucleic Acids Res.* **2006**, *34*, 4225.

[9] a) K. D. Raney, L. C. Sowers, D. P. Millar, S. J. Benkovic, *Proc. Natl. Acad. Sci. USA* **1994**, *91*, 6644; b) L. T. Zhang, G. Schwartz, M. O'Donnell, R. K. Marrison, *Anal. Biochem.* **2001**, *293*, 31.

[10] S. He, B. Song, D. Li, C. Zhu, W. Qi, Y. Wen, L. Wang, S. Song, H. Fang, C. Fan, *Adv. Funct. Mater.* **2010**, *20*, 453.
[11] a) N. Varghese, U. Mogera, A. Govindaraj, A. Das, P. K. Maiti, A. K. Sood, C. N. R. Rao, *ChemPhysChem* **2009**, *10*, 206; b) Z. Liu, J. T. Robinson, X. Sun, H. Dai, *J. Am. Chem. Soc.* **2008**, *130*, 10876; c) R. S. Swathi, K. L. Sebastian, *J. Chem. Phys.* **2008**, *129*, 054703; d) R. S. Swathi, K. L. Sebastian, *J. Chem. Phys.* **2009**, *130*, 086101.
[12] a) A. Bernini, O. Spiga, V. Venditti, F. Prischi, L. Bracci, J. D. Huang, J. A. Tanner, N. Niccolai, *Biochem. Biophys. Res. Commun.* **2006**, *343*, 1101; b) V. Thiel, K. A. Ivanov, A. Putics, T. Hertzig, B. Schelle, S. Bayer, B. Weissbrich, E. J. Snijder, H. Rabenau, H. W. Doerr, A. E. Gorbalenya, J. Ziebuhr, *J. Gen. Virol.* **2003**, *84*, 2305; c) J. A. Tanner, R. M. Watt, Y. B. Chai, L. Y. Lu, M. C. Lin, J. S. M. Peiris, L. L. M. Poon, H. F. Kung, J. D. Huang, *J. Biol. Chem.* **2003**, *278*, 39578.
[13] a) J. D. Huang, B. J. Zheng, H. Z. Sun, *Hong Kong Med. J.* **2008**, *14*, 36; b) N. Yang, J. A. Tanner, Z. Wang, J. D. Huang, B. J. Zheng, N. Y. Zhu, H. Z. Sun, *Chem. Commun.* **2007**, 4413.
[14] Y. J. Jeong, M. K. Levin, S. S. Patel, *Proc. Natl. Acad. Sci. USA* **2004**, *101*, 7264.
[15] L. J. Cote, F. Kim, J. X. Huang, *J. Am. Chem. Soc.* **2009**, *131*, 1043.
[16] a) Z. Luo, Y. Lu, L. A. Somers, A. T. C. Johnson, *J. Am. Chem. Soc.* **2009**, *131*, 898; b) S. Gilje, S. Han, M. Wang, K. L. Wang, R. B. Kaner, *Nano Lett.* **2007**, *7*, 3394; c) N. I. Kovtyukhova, P. J. Ollivier, B. R. Martin, T. E. Mallouk, S. A. Chizhik, E. V. Buzaneva, A. D. Gorchinskiy, *Chem. Mater.* **1999**, *11*, 771; d) H. C. Schniepp, J. L. Li, M. J. McAllister, H. Sai, M. H. Alonso, D. H. Adamson, R. K. Prud'homme, R. Car, D. A. Saville, I. A. Aksay, *J. Phys. Chem. B* **2006**, *110*, 8535.
[17] a) M. Minczuk, J. Piwowarski, M. A. Papworth, K. Awiszus, S. Schalinski, A. Dziembowski, A. Dmochowska, E. Bartnik, K. Tokatlidis, P. P. Stepien, P. Borowski, *Nucleic Acids Res.* **2002**, *30*, 5074; b) K. A. Ivanov, V. Thiel, J. C. Dobbe, Y. V. D. Meer, E. J. Snijder, J. Ziebuhr, *J. Virol.* **2004**, *78*, 5619.
[18] N. R. Bachur, F. Yu, R. Johnson, R. Hickey, Y. Wu, L. Malkas, *Mol. Pharm.* **1992**, *41*, 993.
[19] K. J. Jang, N. R. Lee, W. S. Yeo, Y. J. Jeong, D. E. Kim, *Biochem. Biophys. Res. Commun.* **2008**, *366*, 738.

